Cobalt Telluride Electrocatalyst for Selective Electroreduction of CO_2 to Value-added Chemicals

*Apurv Saxena[a] , Harish Singh[a], Manashi Nath[a]**
[a]Department of Chemistry, Missouri University of Science & Technology, Rolla, MO 65409, USA

Use of widely accepted experimental procedures

We followed data collections methods and protocol as outlined in, "Standards and Protocols for Data Acquisition and Reporting for Studies of the Electrochemical Reduction of Carbon Dioxide" [1] (referred to as Standards paper, hereafter). All our measurements, data collection protocols and reporting follow the guidelines provided in the above-mentioned paper very closely. All our electrochemical experiments have been performed in magnetically stirred solution under rapid bubbling with CO_2 gas to reduce the limitations of mass transfer, as has been suggested in the Standards paper. Limitations to mass transfer can also be reduced by reducing surface roughness of the electrodes and using flat surfaces. All our electrocatalytic experiments have been performed on flat carbon fiber paper electrodes with minimal surface roughness.

As recommended in the Standards paper, we refrained from using Pt as counter electrode to minimize leaching and eventual impurity enrichment in the electrolyte and near the electrode which can lead to unexpected conversions and erroneous data. All our electrocatalytic reactions

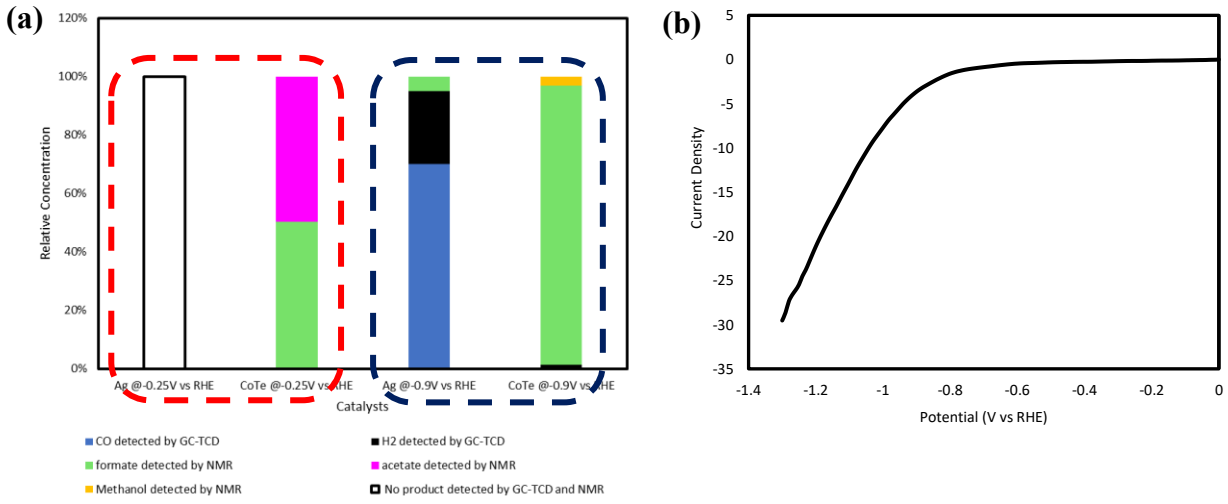

Figure S1. Comparison of CO2RR activity with (a) polycrystalline Ag film synthesized in the authors' lab with CoTe. The polycrystalline Ag tested in the authors laboratory showed formation of CO, HCOOH, and H_2 at -0.9 V vs RHE, while no product was detected with NMR and GC-TCD at -0.25 V (after 2-6 h). The CoTe sample on the other hand, showed distinct presence of acetic acid, ethanol, methanol, and formic acid at -0.9 V, while at -0.25 V it shows exclusive formation of acetic acid. (b) LSV plots of polycrystalline Ag measured in the author's laboratory which matched with that of reported literature

has been performed with glassy carbon as counter electrode. Additionally, we have characterized the electrodes and electrolyte with XRD and ICP-MS which shows the presence of only Co, and Te, and no other impurity atoms confirming purity of the system.

The Standards paper suggested benchmarking of the catalysts by comparing with systems polycrystalline Ag. We calibrated our electrochemical setup by measuring CO2RR activity with polycrystalline silver electrode. Polycrystalline silver electrode in our experimental setup shows similar performance (formation of CO, H_2, and formic acid, at -0.9 V vs RHE applied potential) as has been reported in various studies,[1–3] validating the accuracy of our electrochemical setup. The NMR analysis for products formed from CoTe electrode confirms the presence of methanol and formic acid at -0.9Vin the same setup. Also, the current-density plot of Ag@carbon cloth in presence of CO_2 matches with already done studies (Figure S2 below)[2,3] All our CO2RR experiments were performed in $NaHCO_3$ electrolyte without presence of any other alkali metal ions, which may lead to erroneous data as has been indicated in the Standards paper. We have also reported ECSA and product-specific current density as has been suggested in the Standards paper.

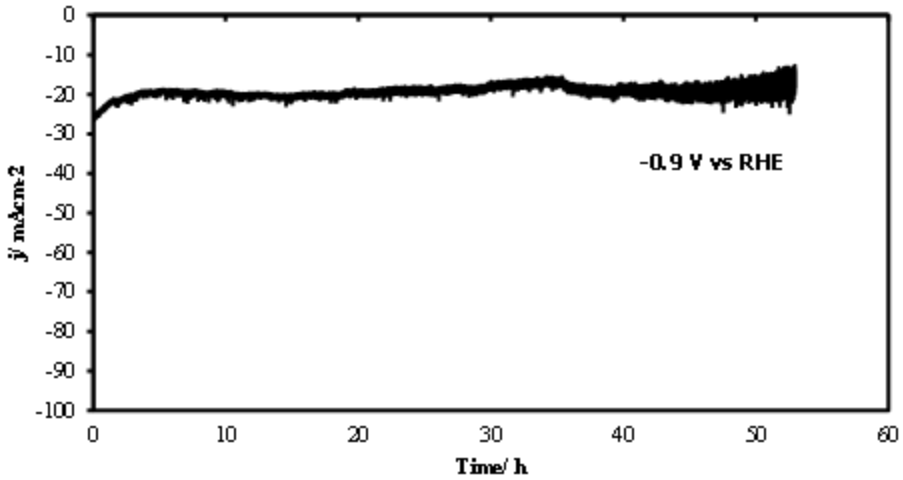

Figure S2. Chronoamperometry study of catalyst for CO_2 electrochemical reduction at fixed potential V = -0.9V vs RHE

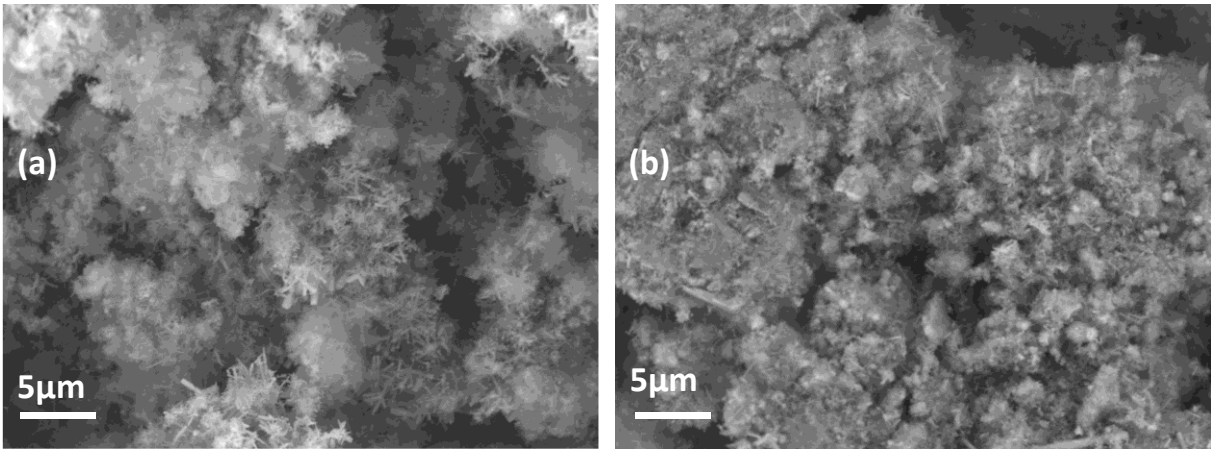

Figure S3. SEM of hydrothermally synthesized CoTe (a) before (b) after CO2RR for prolonged period of time.

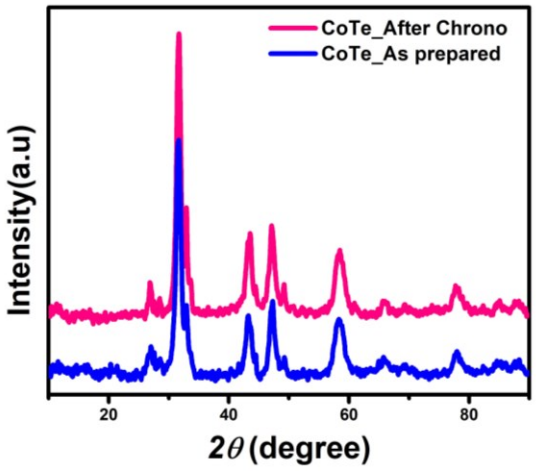

Figure S4. XRD of hydrothermally synthesized CoTe before (blue) and after (pink) CO2RR for 50 h.

Table S1: ICP-MS results from $NaHCO_3$ electrolyte collected at different stages of CO2RR with CoTe		
Sample	Co 59 (ppb)	Te 125 (ppb)
Purified $NaHCO_3$ after 12h CO2RR chronoamperometry with CoTe	<DL	<DL

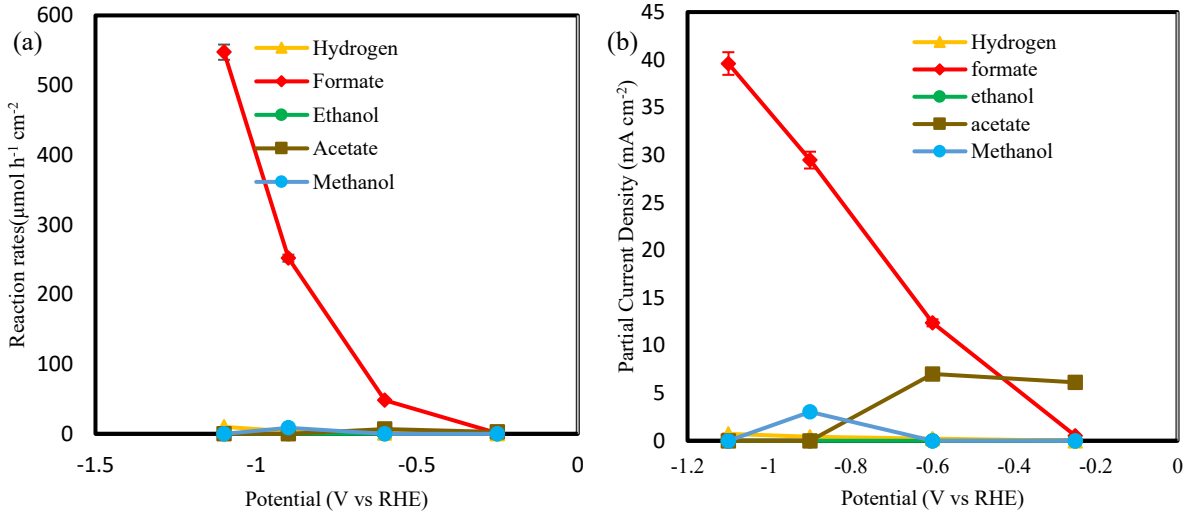

Figure S5. (a) Formation rates with error bars of Hydrogen, formate, ethanol, acetate and methanol at various applied potential. (b) Partial current density with error bars of individual products, hydrogen, formate, ethanol, acetate and methanol at specific potentials.

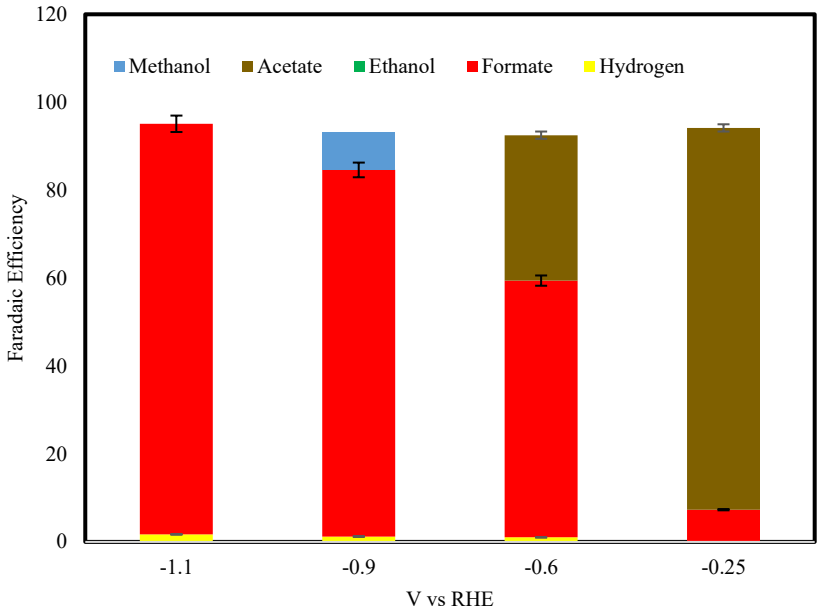

Figure S6. Bar plots with error bars depicting relative faradaic efficiency of cumulative liquid and gas phase CO_2 reduction products at different applied potentials quantified through NMR and GC-TCD.

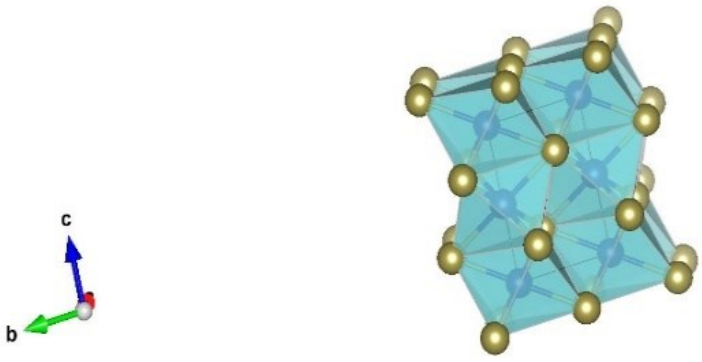

Figure S7. Polyhedral view of the crystal structures of CoTe.

References:

1 E. L. Clark, J. Resasco, A. Landers, J. Lin, L. T. Chung, A. Walton, C. Hahn, T. F. Jaramillo

and A. T. Bell, Standards and Protocols for Data Acquisition and Reporting for Studies of the Electrochemical Reduction of Carbon Dioxide, *ACS Catal.*, 2018, **8**, 6560–6570.

2 W. Qiu, R. Liang, Y. Luo, G. Cui, J. Qiu and X. Sun, A Br− anion adsorbed porous Ag nanowire film: in situ electrochemical preparation and application toward efficient CO2 electroreduction to CO with high selectivity, *Inorg. Chem. Front.*, 2018, **5**, 2238–2241.

3 Y. Yu, N. Zhong, J. Fang, S. Tang, X. Ye, Z. He and S. Song, Comparative Study between Pristine Ag and Ag Foam for Electrochemical Synthesis of Syngas with Carbon Dioxide and Water, *Catal. 2019, Vol. 9, Page 57*, 2019, **9**, 57.

References used in benchmarking figure:

4 Y. Wang, C. Niu, Y. Zhu, D. He and W. Huang, Tunable syngas formation from electrochemical CO2 reduction on copper nanowire arrays, *ACS Appl. Energy Mater.*, 2020, **3**, 9841–9847.

5 W. Ma, S. Xie, X. G. Zhang, F. Sun, J. Kang, Z. Jiang, Q. Zhang, D. Y. Wu and Y. Wang, Promoting electrocatalytic CO2 reduction to formate via sulfur-boosting water activation on indium surfaces, *Nat. Commun. 2019 101*, 2019, **10**, 1–10.

6 A. Aljabour, H. Coskun, X. Zheng, M. G. Kibria, M. Strobel, S. Hild, M. Kehrer, D. Stifter, E. H. Sargent and P. Stadler, Active sulfur sites in semimetallic titanium disulfide enable co2 electroreduction, *ACS Catal.*, 2020, **10**, 66–72.

7 H. Li, X. Liu, S. Chen, D. Yang, Q. Zhang, L. Song, H. Xiao, Q. Zhang, L. Gu and X. Wang, Edge-Exposed Molybdenum Disulfide with N-Doped Carbon Hybridization: A Hierarchical Hollow Electrocatalyst for Carbon Dioxide Reduction, *Adv. Energy Mater.*, 2019, **9**, 1900072.

8 J. Li, X. Xu, B. Huang, Z. Lou and B. Li, Light-Induced in Situ Formation of a Nonmetallic Plasmonic MoS2/MoO3-x Heterostructure with Efficient Charge Transfer for CO2Reduction and SERS Detection, *ACS Appl. Mater. Interfaces*, 2021, **13**, 10047–10053.

9 K. Pellumbi, M. Smialkowski, D. Siegmund and U. P. Apfel, Enhancing the CO2 Electroreduction of Fe/Ni-Pentlandite Catalysts by S/Se Exchange, *Chemistry*, 2020, **26**, 9938.

10 S. Zhao, S. Guo, C. Zhu, J. Gao, H. Li, H. Huang, Y. Liu and Z. Kang, Achieving electroreduction of CO2 to CH3OH with high selectivity using a pyrite–nickel sulfide nanocomposite, *RSC Adv.*, 2017, **7**, 1376–1381.

11 D. Yang, Q. Zhu, C. Chen, H. Liu, Z. Liu, Z. Zhao, X. Zhang, S. Liu and B. Han, Selective electroreduction of carbon dioxide to methanol on copper selenide nanocatalysts, *Nat. Commun. 2019 101*, 2019, **10**, 1–9.

12 X. Liu, H. Yang, J. He, H. Liu, L. Song, L. Li, J. Luo, X. J. Liu, J. He, H. X. Liu, L. D. Song, J. Luo, H. Yang and L. Li, Highly Active, Durable Ultrathin MoTe2 Layers for the Electroreduction of CO2 to CH4, *Small*, 2018, **14**, 1704049.

13 G. Wang, J. Chen, Y. Ding, P. Cai, L. Yi, Y. Li, C. Tu, Y. Hou, Z. Wen and L. Dai, Electrocatalysis for CO2 conversion: from fundamentals to value-added products, *Chem.*

Soc. Rev., 2021, **50**, 4993–5061.

14 X. Yang, P. Deng, D. Liu, S. Zhao, D. Li, H. Wu, Y. Ma, B. Y. Xia, M. Li, C. Xiao and S. Ding, Partial sulfuration-induced defect and interface tailoring on bismuth oxide for promoting electrocatalytic CO2 reduction, *J. Mater. Chem. A*, 2020, **8**, 2472–2480.

15 F. Y. Gao, Z. Z. Wu and M. R. Gao, Electrochemical CO2Reduction on Transition-Metal Chalcogenide Catalysts: Recent Advances and Future Perspectives, *Energy and Fuels*, 2021, **35**, 12869–12883.

16 X. Shao, X. Zhang, Y. Liu, J. Qiao, X. D. Zhou, N. Xu, J. L. Malcombe, J. Yi and J. Zhang, Metal chalcogenide-associated catalysts enabling CO 2 electroreduction to produce low-carbon fuels for energy storage and emission reduction: catalyst structure, morphology, performance, and mechanism, *J. Mater. Chem. A*, 2021, **9**, 2526–2559.